

## REGISTRATION OF NEAR REAL-TIME SAR IMAGES BY IMAGE-TO-IMAGE MATCHING

B. Wessel<sup>a,\*</sup>, M. Huber<sup>a</sup>, A. Roth<sup>a</sup>

<sup>a</sup> German Aerospace Center (DLR), 82234 Weßling, Germany - (birgit.wessel, martin.huber, achim.roth)@dlr.de

Commission IV, WG IV/3

**KEY WORDS:** Disaster, Mapping, SAR, Image, Registration, Orthorectification, Adjustment

### ABSTRACT:

Near real-time SAR images are used at DLRs Center for Satellite Based Crisis Information for mapping natural hazards like flood disasters or landslides. In crisis situations a rapid and precise geocoding is mandatory to produce information within several hours that is comparable with other georeferenced information. Unlikely, the orbit information is often not very precisely known some hours after data acquisition, which leads to misregistration.

This paper deals with the development of a fully automatic orientation for SAR images. The goal is to determine a precise orbit for geocoding by image-to-image matching between a near real-time (NRT) image and a reference SAR image. The approach uses a new algorithm for feature extraction developed in computer vision by Lowe, 2004. No prior information about the pose of the images or the overlapping parts is needed. The point operator extracts points with scale- and rotation-invariant descriptors (SIFT-features). These descriptors allow a successful matching of image points even in situations with highly convergent images, i.e. with different incidence angles. Our approach consists of the following steps: Point extraction and matching by using the SIFT parameter descriptors with an extended matching scheme. The resultant points of the reference image are used as ground control points (GCPs) for an adjustment of the SAR imaging geometry of the NRT image. Then, a geocoding of the NRT SAR image can be carried out. This achieves results equivalent to a high precision orbit.

Examples of two datasets are presented and the results of the approach are discussed and evaluated. The results show that the approach can be used for a wide range of scenes with different SAR sensors, different incidence angles, and different overlap extensions. The results are very reliable but depend on well structured image content.

### 1. INTRODUCTION

One service of DLR is a rapid mapping service in case of larger natural disasters performed by the Center for Satellite Based Crisis Information. Near real-time satellite images are used to map natural hazards like flood disasters or landslides within several hours. As the interpretation often relies on actual and former information a precise geocoding of near real-time satellite data is a mandatory. But due to inaccurate orbit data this is often a difficult task. Inaccurate orbit data leads

- on the one hand to an incorrect geolocation that impede the joint interpretation with other data that often takes place in crisis context.
- On the other hand no correct orthorectification can be performed because the underlying DEM is misaligned to the SAR image. Hence, effects caused by the side looking SAR geometry (layover, foreshortening, shadow) cannot be corrected and so much the worse a misaligned DEM even introduces additional errors during the geocoding process to the SAR image.

The exterior orientation of a SAR image needed for geocoding is established by the sensor trajectory  $S(X,Y,Z)$  over the time  $t$ , the Doppler frequency (if not zero), and the slant range  $R_0$  to the first (near range) pixel. The frequency, time and range information are recorded by the sensor. The knowledge of a high precision orbit is often only several days to one month after the SAR image acquisition available. For recently acquired images mostly just predicted orbits are available.

Though, the predicted orbit of Envisat is within the order of few meters. Especially, RADARSAT orbits generally need substantial refinement as even the post-processing orbit can be shifted by several kilometres. As the overall philosophy in crisis mapping is to be able to process any image one can get, as fast and as good as possible the orbits have to be corrected.

So for near-real time applications some ground control points are needed to solve the sensor trajectory, if the preliminary orbit exceeds the desired accuracy. GCPs can be acquired from maps or other images. Crisis mapping mostly relies on former information, so image-to-image registration is an obvious method for registration. Mostly the GCP measurement is done manually for crisis application. This is a difficult task, as point identification and precise point determination in SAR images is often difficult.

#### 1.1 Overview to related work

Registration of two SAR images is a standard task in InSAR Interferometric co-registration. Standard co-registration technique is based on cross-correlation measure, carried out on extended image patches. This method allows obtaining very high accuracies on image pairs characterized by sufficiently high correlation values. In areas with low coherence or different incidence angles correlation technique results are generally unsatisfactory. Although the normalized cross-correlation is invariant against mean gray-level it is not to local dissimilarities and rotation. To overcome the above limitations, a co-registration approach based on features has been indicated as a

\* Corresponding author.

potential solution. The idea consists of exploiting the response of isolated and bright points to find the image local shifts by estimating their precise position in small patches. Cross-correlation over such small patches provides accurate position estimates (Adam et al., 2003).

The registration approaches for different SAR images like different viewing geometry or different sensors is a difficult topic and currently an ongoing research. An approach quite similar to ours is suggested by Auquière et al., 1998. They perform a simple transformation, i.e. a (2D-)shift, applied to the PRI images. Läbe and Förstner, 2006 used the SIFT operator (Lowe, 2004) for an automatic orientation of aerial images, which is even for optical images still a topic of research.

The development of a mostly automatic procedure for precise geocoding of near real-time satellite SAR images is on our focus in this paper. In the first part of the paper we explain an automatic approach for the generation of ground control points (GCPs) for precise orbit determination. It is based on image-to-image matching with a new developed feature extraction algorithm from computer vision (Lowe, 2004). After GCPs are found a least squares adjustment of the orbit parameters is performed. In the second part of the paper we present some results for this registration method and show in detail the found matches.

## 2. DESIGN OF A PROCEDURE FOR AUTOMATIC GEOCODING BASED ON IMAGE-TO-IMAGE REGISTRATION

We design a registration strategy based on image-to-image registration between a near real-time image and a former SAR image with a post-processing orbit to get precise orbit information. The registration strategy is as follows:

- Getting an archive SAR product with a high-precision orbit, preferred in slant range, e.g. Envisat ASAR
- Getting a near real-time satellite image, e.g. from RADARSAT or Envisat ASAR.
- Extraction of sub-pixel precise interest points in both slant range images with Lowe's SIFT keypoint operator.
- Matching of the keypoints from both images.
- Calculation of the exact 3-D position of the matched keypoints from the high-precision orbit image and a DEM to get GCP's.
- Least squares adjustment of the imprecise orbit by means of the GCPs, including blunder elimination of incorrect matches.
- Final geocoding of the near real-time image on the basis of the refined orbit parameters.

Figure 1. gives an overview of the procedure. In the following the individual steps are discussed in detail.

### 2.1 Input data

Main inputs for the procedure are one geocoded reference image and one near real-time sensed image to be rectified. Here, we focus on registering SAR images. The matching can be performed on geocoded as well as on slant range images. To assure a maximum of similarity, the matching takes place on two slant range images to neglect possible errors. Additionally, required for geocoding is a digital elevation model (DEM) and orbital information. The resolution of the DEM should be in the same order as the aimed image resolution. The orbit

information should be high-precision for the reference image and should be known by approximation for the sensed image.

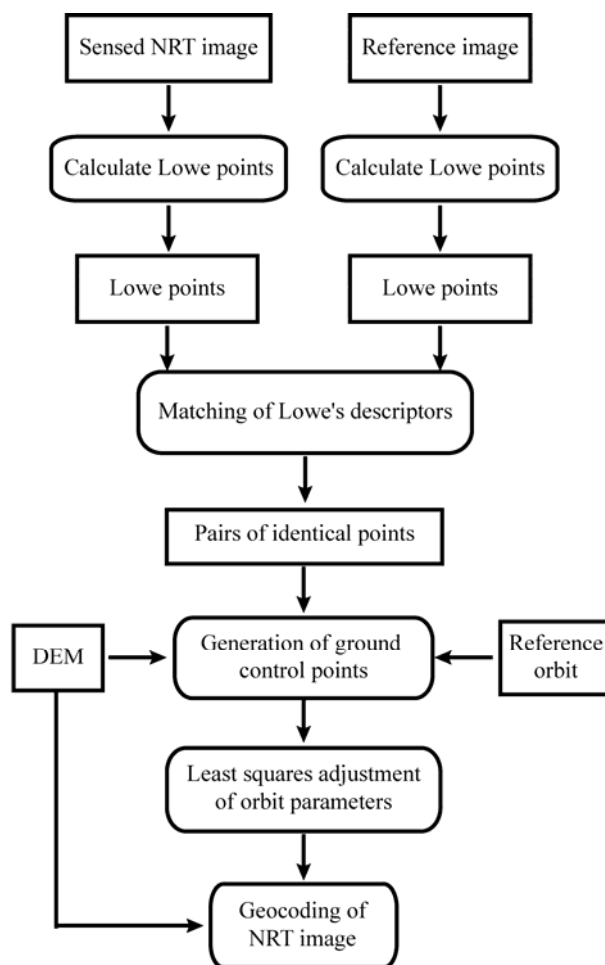


Figure 1. Procedure for automatic geocoding with image-to-image registration. The individual steps are discussed in Sect. 2.

### 2.2 Feature extraction

Generally, significant features are extracted from images to perform a feature matching. Most sophisticated point operators from optical images like the Harris or Förstner operator are not that successful on SAR data, because of the speckle effect. Therefore, for tie-point extraction we chose a newly developed keypoint extractor from Lowe, which was developed for optical images but because of its multi-scale approach it seems especially suitable for SAR data. The computational efficiency and robustness support our task of a fast near real-time geocoding in the same way.

The Lowe keypoint detector (Lowe, 2004) is based on a multi-scale approach and finds scale-independent point features, which are additionally extremely invariant to rotation and affine transformations. Therefore, it can cope with different incidence angles. Samples of found features are presented in Figure 4 and Figure 8.

### 2.3 Feature matching

For matching of two extracted point data sets no further assumptions about the orientation are made. The matching

relies on a vectorial description for each point (Lowe, 2004) and is performed by calculating the Euclidian distance between the vectors. The shorter the distance is, the more likely a homologous point pair is present. The use of that kind of vectorial point description instead of image patches and image correlation allows a very computational efficient and fast matching.

Some additional restrictions are introduced, because incorrect orbit parameters cause mainly shifts in and across the flight direction. So the search space was restricted to a certain distance and to a certain connection angle between a homologous point pair.

**2.4 Generation of GCPs**

The matched feature points have to be transformed into control information by the geometry of the reference image. Input to this transformation is the pixel coordinates resp. slant range coordinates of the homologous points of the reference image, for which typically a high-precision orbit is available. The individual points of the reference image can be geocoded with the help of a DEM and we get 3D-ground control coordinates (= object coordinates) of the corresponding points. These can be used as ground control points for adjusting the orbit parameters.

**2.5 Least squares adjustment of orbit parameters**

The next step is an adjustment for determining the near real-time orbit with the help of GCPs. A classical least squares adjustment is performed to estimate the unknown orbit parameters.

The position of the sensor depends on the time. It can be approximated locally with high accuracy by an orbit polynomial, which is derived from annotated sensor positions (state vectors). The functional model is described in the following.

**Functional model for orbit determination:** The equations used for the adjustment are the same used for geocoding. To be demanded are the parameters of the orbit polynomial that is approximated by a polynomial of forth degree

$$S(i) = \vec{a}_0 + \vec{a}_1i + \vec{a}_2i^2 + \vec{a}_2i^3 + \vec{a}_2i^4 \tag{1}$$

with  $S = [X_S, Y_S, Z_S]$  = coordinates of the sensor  
 $i$  = azimuth/time

The Doppler and range equations give the relation between ground and image coordinates in a SAR image (see Figure 2 or Roth et al., 1993):

$$F_1(i, j) = f_{DC} - \frac{2(\vec{P} - \vec{S})(\vec{P}' - \vec{S}')}{\lambda |\vec{P} - \vec{S}|} \tag{2}$$

$$\vec{R} = \|\vec{P} - \vec{S}\|$$

$$F_2(i, j) = R_0 + m_r j - |\vec{P} - \vec{S}| \tag{3}$$

- where  $i, j$  = image coordinates ( $i$ : azimuth/time;  $j$ : range)
- $\vec{P} = [X, Y, Z]$  = coordinates of mapped pixels on earth ellipsoid
- $R$  = slant range vector between sensor  $S$  and earth location  $P$
- $\vec{P}', \vec{S}'$  = velocity of  $P$  resp.  $S$
- $\lambda$  = radar wavelength
- $f_{DC}$  = Doppler frequency shift
- $R_0$  = slant range to first image row
- $m_r$  = pixel spacing

As the orbit is only approximately known for real-time applications the adjustment solves iteratively the radar equations (Eqs. 2 and 3) by adjusting the orbit polynomial until the range and Doppler equations are simultaneously fulfilled. The adjustment contains a blunder elimination that eliminates those GCPs from the calculation that derivation is significant greater than the standard deviation of the iteration result. When the iteration result is found the adjusted orbit can be used for geocoding.

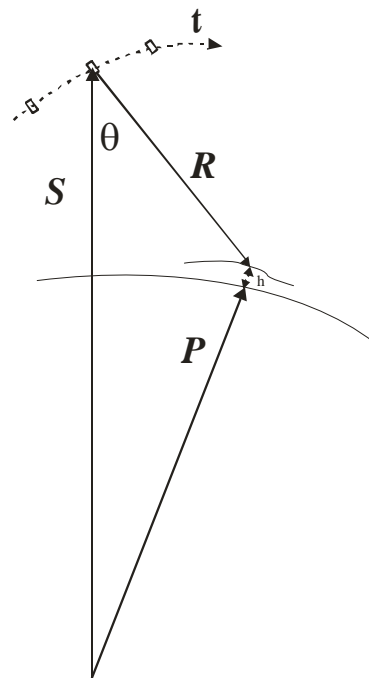


Figure 2. Functional sensor model of the SAR acquisition.

**2.6 Geocoding of near-real time image**

The last step of the procedure is to geocode the sensed NRT SAR image with the help of the adjusted orbit parameters. For geocoding the indirect rectification method is used. For each output pixel, which defines a co-ordinate triple (easting, northing, height) in the output map projection, the corresponding azimuth and range positions in the input image are determined. The Equations (1) to (3) are used for this step. The geocoding can be performed by means of interpolative or rigorous approach, respectively (Huber et al., 2004, Roth et al., 1994).

Note, that with the described method for image-to-image registration no previously known GCPs or manual measured GCPs are necessary.

### 3. EXAMPLES FOR NEAR REAL-TIME GEOCODING

The procedure has been applied to various SAR data sets as well as to aerial optical images. The tests presented here stem from a high-resolution aerial SAR data set and from a real crisis data set in Lebanon. The tests are carried out with a demonstration version of the Lowe keypoint extractor (<http://www.cs.ubc.ca/~lowe/keypoints/>). This version is restricted to images with a maximum image height or width of 1800 pixel. Therefore, we reduced the SAR images by a factor of eight instead of using the original image sizes. But as the points are extracted sub-pixel precise the loss of accuracy was smaller than expected. Also image reduction corresponds to a filtering and therefore reduces the speckle.

#### 3.1 Matching of multi-temporal images

The first test site is based on two E-SAR images. The images were acquired in August 2002 and March 2003 and show the DLR in Oberpfaffenhofen, Germany. Both are acquired with almost the same incidence angles and overlap 100 %, though the reference image covers a larger scene. For the near real-time approach it is assumed that a high-precision orbit is only available for the first image. The extraction of Lowe points is done in slant range geometry. The resolution is reduced by a factor of eight that corresponds to a multilooking of eight pixels and a pixel spacing of about 8 m.

Figure 3 shows a closer view on some matched keypoints to demonstrate which kind of points are extracted and matched. The found corresponding points are mainly brighter or darker than its surroundings. Points 1 and 2 in Figure 3 are at the border of a darker to a brighter image region. Point 3 in Figure 3 is a round dark feature. As the extractor works in multiple scales all points are singular at a specific scale. One can note that by the bright keypoint 4, obviously it has significance in a smaller image scale.

The total number of extracted keypoints is above 1.000 for each image. The number of matched points is 75. Remarkable is the reliability of the matches. Nearly all found matches are correct. Only one mis-match is present (Figure 5). In Figure 5 the 75 matched keypoints are overlaid on the two images. Each keypoint pair is connected by a line. Correct matches are characterized by parallel lines. The amount of 75 was sufficient to solve the Eqs 1, 2, and 3 and to adjust the orbit of the second E-SAR image. The result of geocoding with the adjusted orbit is shown in Figure 4. Its accuracy is within half a pixel (0.5 m). Though, the keypoint extraction took place on 8 m pixel. This emphasizes the subpixel capability of the Lowe operator.

#### 3.2 Matching of images with different incidence angle and from different sensors

The second test site is located in Lebanon and stem from a real crisis charter call to detect the oil spill in August 2006. The terrain is hilly to mountainous (see Figure 6). For this test site ENVISAT and RADARSAT images are available. This test site is more difficult than the previous since the images

- are from different sensors,
- have different incidence angles (22° - ENVISAT resp. 45° - RADARSAT), and
- the overlap is about 50% but without the water areas just 25 %.

Nevertheless, 6 matches were found. Figure 8 shows in detail the found matching partners between the Envisat and the Radarsat image.

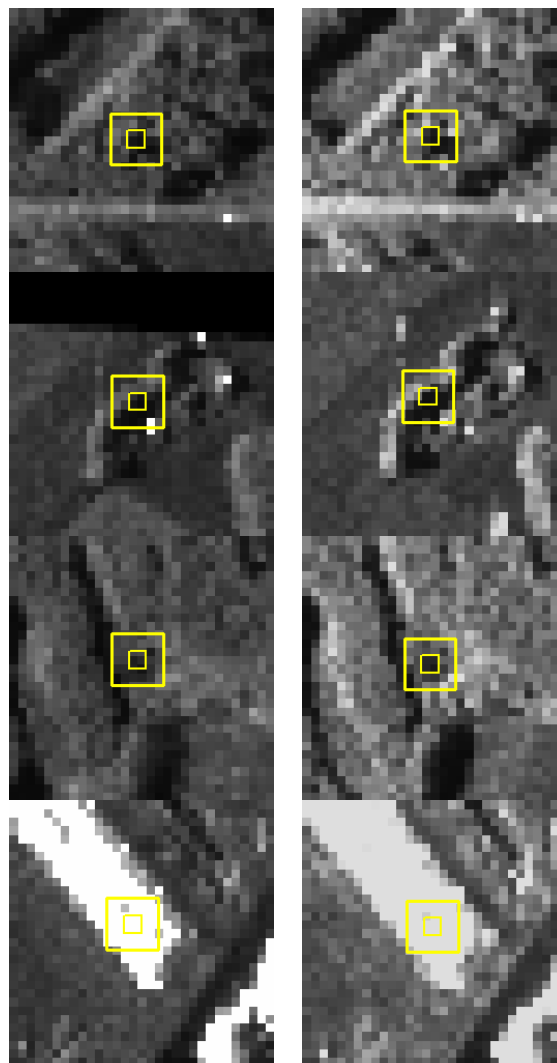


Figure 3. Left the new “near real-time” E-SAR image right reference image

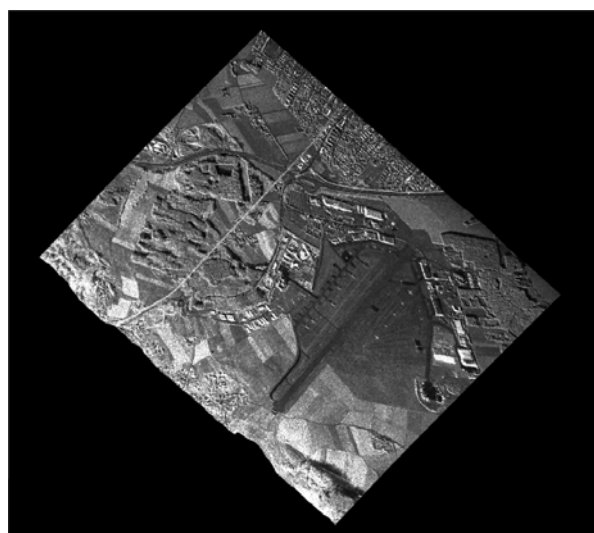


Figure 4. Geocoded E-SAR image by an adjusted orbit based on image to image registration

Though, the dimensions of the found features are different, the detection of features darker or brighter than its surrounding is equal to the behaviour of the high-resolution keypoints.

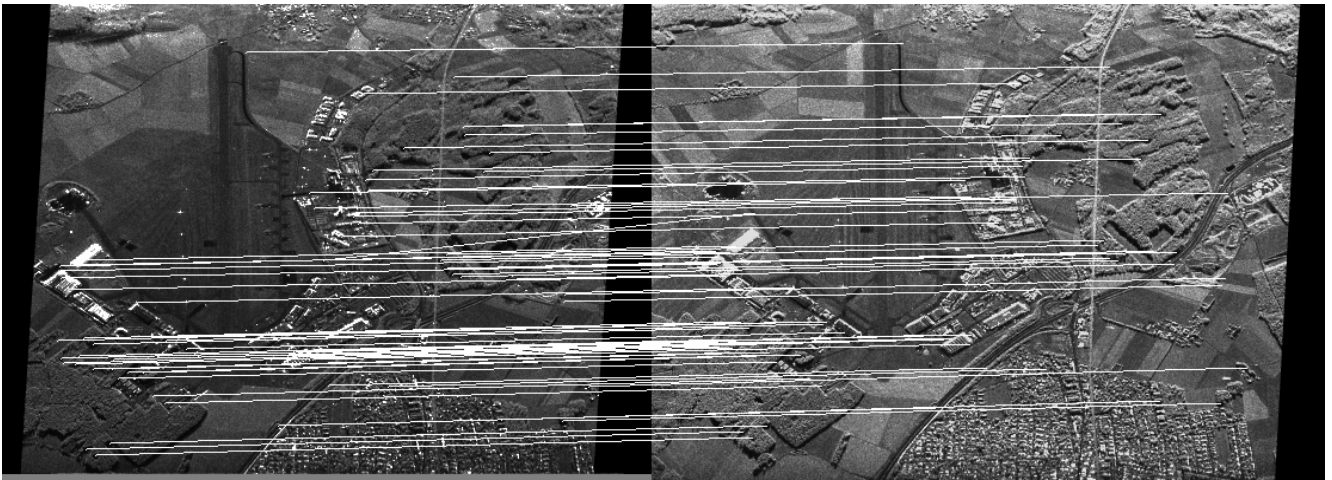


Figure 5. Results of matched SIFT keypoints on two E-SAR scenes in slant range geometry. The white lines connect two matched keypoints with each other: on the left the new “near real-time” E-SAR image on the right the reference image. 75 Matches were found.

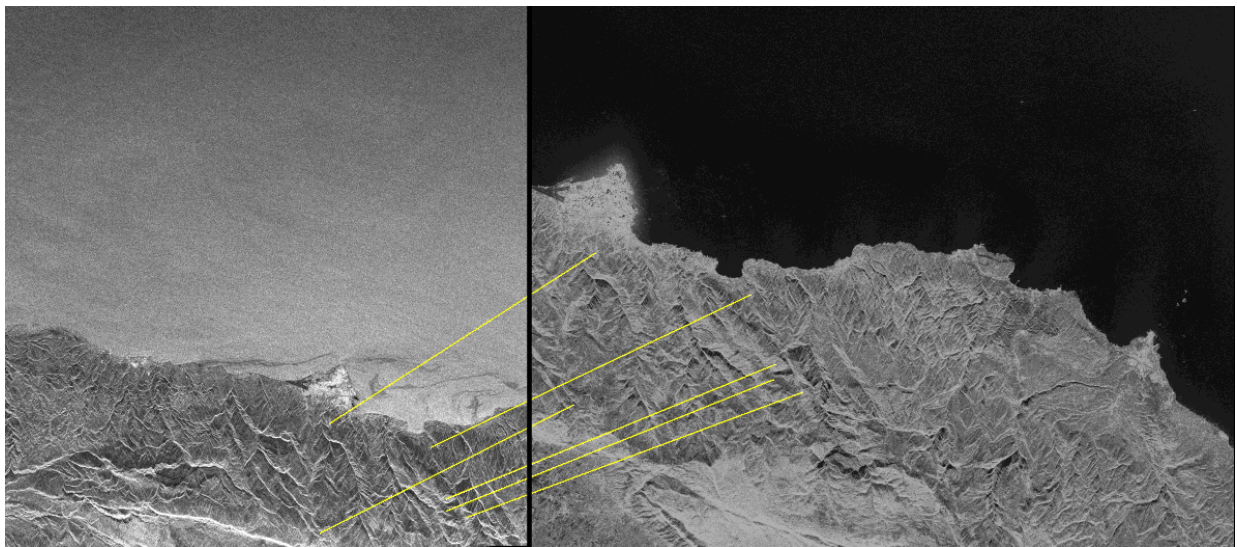


Figure 6. Lebanon test site results of matched SIFT keypoints between an ENVISAT scene (left) and a RADARSAT scenes (right) in slant range geometry. The yellow lines connect two matched keypoints with each other. 6 Matches were found.

But for reliable orbit determination a larger amount of GCP's would be necessary. At least more than 9 points are needed for orbit determination. As this wasn't possible in the test scene, no adjustment of SAR geometry was possible.

But such a limited number of points still can be used for a coarse image registration. The concept of a two-stage registration is fairly spread in optical image registration. At a reduced resolution some good points for a coarse registration are extracted and e.g. the coefficients of an affine transformation are calculated. Then, a fine matching takes place. Such a registration strategy, i.e. a two-stage registration, can be highly recommended for matching of SAR data. First of all, this technique is successfully used in optical data registration procedures. Secondly, it has the great advantage for SAR images that in very coarse resolution the speckle almost cancels out. And thirdly, for SAR data does a large amount of fine registration techniques from InSAR exist, which necessarily need good coarse registration.

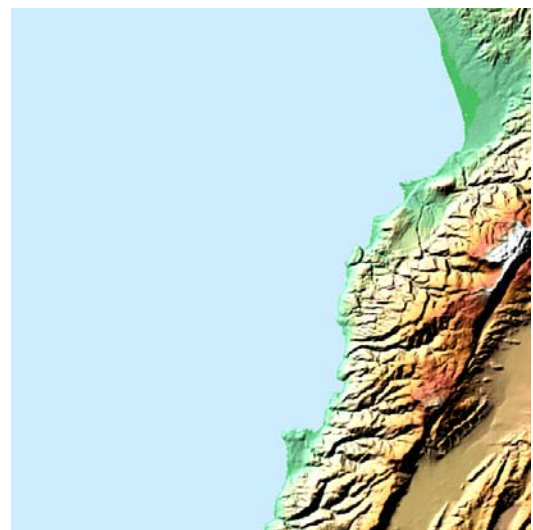


Figure 7. Digital elevation model of the Lebanon test site.

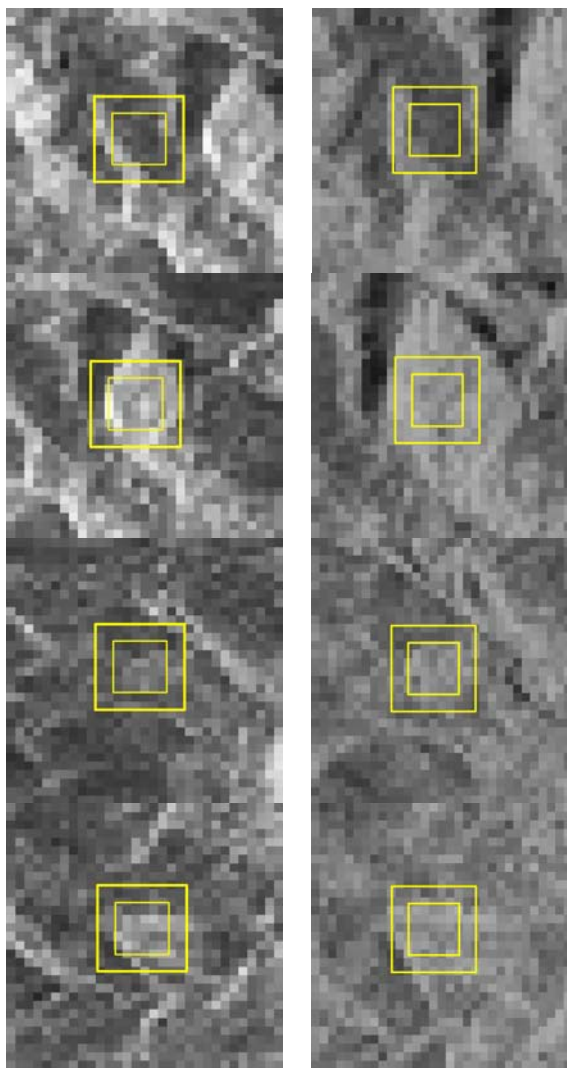


Figure 8. Examples of four extracted and matched SIFT image pairs from RADARSAT (left) versus ENVISAT (right)

#### 4. SUMMARY AND OUTLOOK

The goal of the presented procedure aims to an automatic geocoding of near real-time images for crisis applications. The registration strategy relies on image-to-image matching of SAR images on the basis of the newly developed Lowe feature extractor. The results presented show that the Lowe operator performs surprisingly well on SAR images. In high resolution E-SAR images with forested and urban structures sufficient keypoints could be extracted to perform an adjustment of the orbit geometry for geocoding. The matches are characterized by very high reliability with a small rate of mismatches. Also on strongly different images with different incidence angles, different orbits and different sensors (ENVISAT versus RADARSAT) some reliable matches could be found in mountainous areas. Although the number was too low for orbit determination, the results are promising since the Lowe keypoint extraction is very fast and robust. One drawback seems that the keypoint operator strongly depends on well structured image content.

Further investigations on a refined strategy for keypoint extraction into a separated coarse and fine registration like it is used for optical images will be carried out. Also a matching

with the DEM will be investigated. For low structured scenes additional features like lines or contours should be extracted to improve the registration.

#### REFERENCES

- Adam, N., Kampes, B., Eineder, M., Worawattanamateekul J., and Kircher, M. 2003. The development of a scientific permanent scatterer system. In: *Proceedings of the ISPRS/EARSel Workshop "High Resolution Mapping from Space"*, Hannover (Germany)
- Auquière, E., Hau, P & Defourny, P. (1998). A fast track geocoding method for high temporal resolution SAR time series. In: *Proceedings of the Workshop on "Retrieval of Bio- and Geo-Physical Parameters from SAR Data for Land Applications"*, 21.-23. October 1998, ESTEC, Noordwijk, The Netherlands
- Huber M., Hummelbrunner W., Raggam H., Small D., Kosmann D. (2004), Technical Aspects of Envisat-ASAR Geocoding Capability at DLR. In: *Proceedings of the ENVISAT/ERS Symposium*, Salzburg, Austria, 6-10 September 2004.
- Läbe; T., Förstner, W, 2006. Automatic relative orientation of images. In: *Proceedings of the 5th Turkish-German Joint Geodetic Days*, March 29th – 31st, 2006, Berlin.
- Lowe, D., 2004. Distinctive image features from scale-invariant keypoints. In: *International Journal of Computer Vision*, 60(2), pp. 91-110.
- Lowe, D. 2005. SIFT demo program, Version 4, July 2005, <http://www.cs.ubc.ca/~lowe/keypoints/> (accessed 11 Jul. 2007)
- Roth, A., Craubner, A, Hügel, T., 1993. Standard geocoded ellipsoid corrected images. In: Schreier G. (Ed.): *SAR Geocoding and Systems*, Wichmann, Karlsruhe, pp. 159-172.
- Roth A., Huber M., Kosmann D. (2004), Geocoding of TerraSAR-X Data. In: *Proceedings of the 20th International Congress of the ISPRS*, Istanbul, Turkey, 12-23 July 2004, Commission III, pp. 840-844.